



Supplementary Materials for

Meissner corpuscles and their spatially intermingled afferents underlie gentle touch perception

Nicole L. Neubarth^{1,2,*}, Alan J. Emanuel^{1,2,*}, Yin Liu^{3,*}, Mark W. Springel^{1,2}, Annie Handler^{1,2}, Qiyu Zhang^{1,2}, Brendan P. Lehnert^{1,2}, Chong Guo¹, Lauren L. Orefice^{1,2}, Amira Abdelaziz^{1,2}, Michelle M. DeLisle^{1,2}, Michael Iskols^{1,2}, Julia Rhyins^{1,2}, Soo J. Kim^{1,2}, Stuart J. Cattel^{1,2}, Wade Regehr¹, Christopher D. Harvey¹, Jan Drugowitsch¹, and David D. Ginty^{1,2}

¹Department of Neurobiology, ²Howard Hughes Medical Institute, Harvard Medical School, 220 Longwood Avenue, Boston, MA 02115

³Department of Biochemistry, Howard Hughes Medical Institute, Stanford University, 279 Campus Drive, Stanford, CA 94305

⁴Present address: Two Six Labs, 901 North Stuart Street, Arlington, VA 22203, USA

*equal contributions

Correspondence to: david_ginty@hms.harvard.edu

This PDF file includes:

Materials and Methods
Figs. S1 to S10
Captions to Movies S1 and S2
References (30-43)

Other Supplementary Materials for this manuscript include the following.

Movies S1 and S2

Materials and Methods

Animals

Animals were handled according to protocols approved by the Harvard Standing Committee on Animal Care and are in accordance with Federal guidelines.

Mouse lines

The *TrkB^{flox}*, *Advillin^{Cre}* (JAX 032536), *K5Cre* (MGI 3050065), *Atoh1^{flox}* (JAX 008681), *Ret^{CreER}* (MGI #4437245), *Ai14* (*Rosa26^{LSL-tdTomato}*; JAX 007914), *Ret^{CFP}* (MGI 3777555), *Npy2r-GFP* (MGI 3844094), *Rosa26^{iAP}* (JAX 009253), *Ai3* (*Rosa26^{LSL-YFP}*; JAX 007903), *Ai32* (*Rosa26^{LSL-ChR2(H134R)-EYFP}*; JAX 024109), *TrkB^{CreER}* (JAX 027214), *Pvalb^{2A-FlpO-D}* (JAX 022730), *Ai65* (*Rosa26^{FSF-LSL-tdTomato}*; JAX 021875), *Rosa26^{LSL-FSF-ReaChR-mCitrine}* (JAX 024846), *Rosa26^{DR-Matrix-dAPEX2}* (JAX 032764), *Rosa26^{LSL-Matrix-dAPEX2}*, *Brn3a^{f(AP)}* (JAX 010558), *BDNF^{lacZ}* (*BDNF^{flox}*; JAX 021055), *Wnt1Cre* (JAX 022137), and *DhhCre* (JAX 012929) mouse lines have been described previously (5, 6, 9, 14, 15, 17-20, 28, 30-38). The *Advillin^{FlpO}* mouse line, which was generated by standard gene targeting procedures, enables FlpO-dependent recombination in somatosensory and other peripheral nervous system neurons and will be described in detail elsewhere. All lines were kept on a mixed CD1-C57Bl/6 background.

Tamoxifen Treatments

Tamoxifen (Toronto Research Chemicals) was dissolved in 100% ethanol (20mg/mL). The tamoxifen/ethanol mixture was diluted with sunflower seed oil (Sigma) at a 1:2 dilution and vacuum centrifuged for 30-45 minutes until the ethanol evaporated. The resulting solution was

stored at -20°C and thawed immediately prior to use. For embryonic tamoxifen treatment, the oil/tamoxifen solution was delivered to pregnant mothers via oral gavage. The Ret⁺ Meissner afferent population was labeled with high efficiency by giving pregnant mother a 2 mg dose of tamoxifen at E11.5 and E12.5. The forelimb was labeled more effectively at E11.5, while the hindlimb was labeled more effectively at E12.5. The TrkB⁺ Meissner afferent population was labeled with high efficiency using intraperitoneal (IP) injection of P4 pups (0.5 mg), but this population was also labeled when pregnant mothers were given tamoxifen any time between E12.5 and E16.5 and when P5 pups were given 0.5 mg of tamoxifen.

Immunohistochemistry

P20 or older mice were euthanized with CO₂ and perfused with Ames Media (Sigma) containing 10 U/mL heparin (Sigma) in PBS, followed by 4% paraformaldehyde (PFA) in PBS. Spinal cords and brainstems were dissected and fixed in 4% PFA at 4 °C overnight. For skin sectioning experiments, glabrous toe and pedal pads were removed from the paw and placed in 4% PFA for 4-6 hours or Zamboni's fixation buffer for 24-48 hours at 4 °C. For whole-mount immunohistochemistry, whole paws were placed in Zamboni's fixation buffer at 4 °C for 24-48 hours. The glabrous skin was then separated from the underlying tissue via fine dissection in PBS. Isolated glabrous paws were fixed in Zamboni's fixation buffer for an additional 1 hour at room temperature. Following fixation, all tissues were rinsed 3x10 minutes in PBS at room temperature. Brainstems and spinal cords with dorsal root ganglia attached were isolated from the vertebral column.

Glabrous pads, spinal cords, and brainstems destined for sectioning were cryoprotected in 30% sucrose in PBS at 4 °C for 24-48 hours. Tissues were embedded in OCT (Tissue Tek) and frozen at -20 °C. Glabrous pads were sectioned at 25 µm, and spinal cords and brainstems were sectioned transversely at 40-50 µm. Sections were dried overnight at room temperature. Glabrous pads were given 1-2 additional days to dry. All sections were rinsed 3x10 minutes with PBS, blocked with 5% normal serum (donkey or goat) in 0.1% PBST (0.1% Triton X-100 in PBS) for 2 hours, and incubated with primary antibody in blocking solution overnight at 4 °C. The following day, sections were rinsed 3x10 minutes with PBST and incubated with secondary antibodies in blocking solution for 2 hours at room temperature or overnight at 4 °C. Sections were then rinsed 1x10 minutes in PBST and 2x10 minutes in PBS and mounted with Fluoromount-G (Southern Biotech). Images were acquired on a Carl Zeiss LSM 700 confocal microscope.

Whole-mount immunohistochemistry of glabrous skin was performed as described previously (7). The skin was given several one-hour washes in 0.3-0.5% TritonX-100 in PBS. The skin was then incubated in primary antibodies in blocking solution (5% normal serum (goat or donkey), 75% PBST, 20% DMSO) at room temperature for 72 hours. The skin was washed in PBST for 4-5x1 hour and incubated in secondary antibodies in blocking solution at room temperature for 48 hours. Tissue was washed several times in PBST then dehydrated in serial methanol dilutions (1 hour each of 25%, 50%, 75%, and 100%), followed by overnight dehydration in 100% methanol at room temperature. The tissue was then cleared in BABB (1 part Benzyl Alcohol: 2 parts Benzyl Benzoate) and imaged.

Primary antibodies were rabbit anti-DsRed (Clontech, Cat. # 632496, 1:500), goat anti-mCherry (Sicgen, Cat. # AB0040-200, 1:500), chicken anti-GFP (Aves Lab, Cat. # GFP-1020, 1:500), rabbit anti-GFP (Invitrogen, Cat. # A-11122, 1:500), goat anti-GFP (US Biological, Cat. # G8965-01E, 1:500), rat anti-MBP (Millipore, Cat. # MAB386, 1:500), rabbit anti-NFH (Sigma, Cat. # N4142, 1:1000), chicken anti-NFH (Aves Lab, Cat. # NFH, 1:500), rabbit anti-S100 (Dako, Cat. # Z031129-2, 1:300), rabbit anti-PKC γ (Santa Cruz, Cat. # SC-211, 1:500), and TROMA-I (rat anti-keratin 8/cytokeratin 18, DSHB, University of Iowa, TROMA-I supernatant, 1:100). The nucleic acid stain TO-PRO-3 (Invitrogen, Cat. # T3605, 1:500), the nonpeptidgeric nociceptor marker IB4 (Isolectin GS-IB₄, conjugated to Alexa Fluor 647, Life Technologies, Cat. # I32450, 1:500), and the nucleic acid stain Hoechst 33258 (Fisher, Cat. # H3569, 1:1000) were applied during secondary antibody incubation.

X-gal staining

Embryos and glabrous skin were fixed with a glutaraldehyde solution (0.2% glutaraldehyde, 2 mM MgCl₂ in PBS) overnight at 4 °C. For whole-mount staining, fixed embryos or skin were washed with detergent rinse buffer (0.01% sodium deoxycholate, 0.02% NP40, 2 mM MgCl₂ in phosphate buffer, pH 7.4) and stained with staining buffer (0.01% sodium deoxycholate, 0.02% NP40, 2 mM MgCl₂, 5mM potassium ferricyanide, 5mM potassium ferrocyanide, 1mg/ml 5-bromo-4-chloro-indolyl- β -D-galactopyranoside in phosphate buffer, pH 7.4) at room temperature. After staining, embryos were dehydrated sequentially with 50% methanol, 80% methanol, and 100% methanol. For staining on sections, 12 μ m sections were cut and dried for

several hours at room temperature. The staining procedure was the same as described for whole-mount staining. After staining, sections were fixed overnight at 4 °C in 4% PFA in PBS, and mounted with Fluoromount-G.

Fluorescent Sparse Labeling

TrkB⁺ Meissner afferents were sparsely labeled by injecting the pedal pads of TrkB^{CreER}; Ai65 mice with a viral vector containing FlpO recombinase, AAV1-hSyn-FlpO (AAV2/1.humanSynapsin1.FlpO.bGH, UPenn Vector Core, titer = 1.23×10^{13} gc/ml). Mice were administered 0.5 mg of tamoxifen at P5 via IP injection. Mice aged P9 were anesthetized via isoflurane (2-3%) delivered from a precision vaporizer. Animals were monitored throughout the 5-10 minute procedure, and the anesthetic dose was adjusted as necessary. AAV1-hSyn-FlpO combined with a small amount of Fast Green dye (Sigma F7252-5G) in 0.9% saline was injected into 1-3 hindlimb or forelimb pedal pads per animal via a beveled glass capillary needle (FHC Inc capillary tubing, FHC 27-30-0). The total volume of AAV/Fast Green mixture injected per pad for sparse labeling was approximately 0.1-0.5 μ l. Mice were removed from anesthesia, administered analgesic (Carprofen, 4 mg/kg), and placed on a warm pad for recovery. Animals were given an additional dose of Carprofen after 24 hours and observed to ensure adequate recovery. Mice were perfused 2-9 weeks after injection, and their vertebral columns and glabrous paws were prepared as described above. The viral dose was titrated to achieve labeling of a single neuron per animal, and only mice in which a single cervical or lumbar neuron was observed in the DRG were included in subsequent analyses.

Alkaline Phosphatase Histochemistry

Placental alkaline phosphatase (PLAP) staining was performed as described previously (6).

Whole paws from P21 mice were fixed in Zamboni's fixation buffer at 4 °C for 24-48 hours. Age was kept consistent to prevent age and size differences from contributing to observed differences between Ret⁺ Meissner afferent and TrkB⁺ Meissner afferent receptive fields. The glabrous skin was then separated from the underlying tissue via fine dissection in PBS. Isolated glabrous paws were fixed in Zamboni's fixation buffer for an additional 1 hour at room temperature. Following fixation, all tissues were rinsed 3x10 minutes in PBS at room temperature and then incubated at 65-68 °C for 2 hours. To detect PLAP signal, tissues were incubated with BCIP/NBT (Roche) solution (diluted in 0.1 M Tris pH 9.5, 0.1 M NaCl, 50 mM MgCl₂, 0.1% Tween-20 solution) overnight at room temperature. Tissues were then fixed in 4% PFA in PBS for 1 hour at room temperature, followed by dehydration in ethanol (1 hour 50%, 1 hour 75%, 1 hour 100%, overnight 100%). Finally, tissues were cleared in BABB and imaged.

To sparsely label Ret⁺ Meissner afferents, pregnant mice were administered 1 mg tamoxifen at either E11.5 or E12.5. For TrkB⁺ Meissner afferents, pregnant mice were administered 1 mg tamoxifen at E14.5.

Quantification of Receptive Field Geometries

Images of Meissner afferent terminal arborizations in glabrous pads were analyzed in the Fiji distribution of ImageJ (www.fiji.sc). The perimeter of individual receptive fields (terminal area) was outlined by hand, and the resulting selection was subjected to the Convex Hull function,

which replaces a polygon with its convex hull. The area in μm^2 and the aspect ratio (major axis/minor axis) of the convex hull were measured using the measure function. Terminals of afferent arborizations were counted by eye. For some neurons, two fibers from the same neuron could be seen traveling together and terminating in the same corpuscle. In these cases, the two fibers were counted as a single termination. This phenomenon appeared to occur more often for TrkB⁺ Meissner afferents than for Ret⁺ Meissner afferents, but this was not quantified.

In Vivo Electrophysiological Recordings

In vivo dorsal root ganglia (DRG) recordings were made as described previously (7) using a preparation modified from that published by Ma, Donnelly and LaMotte (8). Ret^{CreER} or TrkB^{CreER} mice with a Cre-dependent YFP, tdTomato, or mCitrine reporter (Ai14, Ai32, or Rosa26^{LSL-RedChR-mCitrine}) were administered tamoxifen at the appropriate ages. Since this strategy also labels hairy-skin-innervating neurons, we anterogradely labeled glabrous neurons via subcutaneous injection of cholera toxin subunit B conjugated to Alexa 555 or Alexa 488 (Thermo Fisher; 2 $\mu\text{g}/\mu\text{l}$ in PBS, approximately 0.3 μl per pad) into the left hindlimb toe and pedal pads 2-3 days prior to recording. On the day of recording, P20-P60 mice were anesthetized with urethane (1 g/kg) via intraperitoneal injection. Anesthesia was maintained with isoflurane (1.5-2% in 100% O₂) for the duration of the surgery and subsequent recording period (SomnoSuite, Kent Scientific). Mouse internal temperature was monitored via a rectal probe and maintained at 35.5-37.5 °C with a temperature controller (TC-344B, Warner Instruments) and thermoelectric heater (C3200-6145, Honeywell) embedded in castable cement (Aremco). The lumbar vertebral column was exposed and secured with custom spinal clamps (Mike's Machine, Attleboro MA).

Bone dorsal to the target DRG(s) (L3-L5) was removed with rongeurs. The surgical site was continuously perfused with and immersed in external solution containing (in mM) 140 NaCl, 3.1 KCl, 0.5 KH₂PO₄, 6 glucose, 1.2 CaCl₂, 1.2 MgSO₄, and 10 HEPES. pH was adjusted to 7.4 with NaOH. The epineurium surrounding the DRG was removed with fine forceps. The DRG was visualized using custom reflective optics on an upright compound microscope (Zeiss). Cell bodies on the surface of the DRG were accessible for recording. Borosilicate glass pipettes (TW150F-4, WPI) were pulled to achieve a 20-30 μm tip diameter. Pipettes were then filled with external solution, and fluorescent cell bodies that were labeled with dye-conjugated CTB were targeted for cell-attached recordings.

Neuron receptive fields (RFs) were localized using a small paintbrush and gentle manual probing. For Meissner afferents, RFs were confined to single toe or pedal pad in the hindlimb. To estimate conduction velocity (CV), an electrical stimulus was delivered to the RF using a bipolar electrode. The delivered current was 2.5 times the threshold at which the neuron fired an action potential. CVs were estimated by dividing the conduction latency (average latency out of 10 trials) by the distance between the DRG and the RF. This distance did not account for the tortuosity of the sensory axon, and, thus, the reported CVs are a lower-bound on the true value. Force-controlled indentation of skin was achieved using an indenter (Model 300 C-I, Aurora Scientific) mounted on two orthogonal linear motorized stages (MTS25/M-Z8E, Thorlabs). The XY position of the indenter was controlled using the stages. The indenter was positioned on top of the RF such that the tip of the indenter was barely touching the surface of

the glabrous pad. Sinusoidal force stimuli and low-pass filtered (15 ms boxcar) force steps were synthesized in MATLAB (Mathworks, Natick, MA) and delivered to the skin.

For random recordings of A β -LTMRs that innervate glabrous skin (Figure 1), the hindpaw glabrous skin pedal pads of *TrkB^{flox/flox}* controls and *TrkB^{CKO}* mice were injected with CTB conjugated to Alexa 488 24-72 hours prior to recording. Neurons with large soma diameters (> 25 μ m) that contained CTB 488 were targeted for recording. The receptive fields of the neurons were localized with manual brushing, and force indentations (0.5 s duration, 1-75 mN intensity) were applied to the receptive field. RA neurons were defined as those with spiking responses to indentation at only the onset or offset of the step indentation. SA neurons were defined as those with spikes occurring at the onset and the middle of the step indentation. SA neurons never increased their firing rate in response to the termination of the indentation. Non-responsive (NR) neurons were defined as those that produced action potentials in response to stretching of the foot, but not to the indentation. Extracellular action potentials were recording using a Multiclamp 700A amplifier (Axon Instruments) operating in the voltage-clamp configuration, which was constantly adjusted so that no current was passed by the amplifier. Electrophysiological data was digitized at 40 kHz by a 16-bit A/D converter (USB-6259, National Instruments), low-pass filtered at 10 kHz using the amplifier's internal four-pole Bessel filter, and acquired using pClamp. All electrophysiological data were analyzed using custom Python scripts.

Quantification of Meissner Corpuscle and Merkel Complex Density

Images of serial sections of glabrous pads were sectioned at 25 μm . Images of sections were analyzed in the Fiji distribution of ImageJ (www.fiji.sc). In each section, the number of Meissner corpuscles, visualized via S100 antibody (Meissner corpuscles formed large, ovoid masses in the dermal papillae compared to Schwann cells surrounding neurons, which are also S100⁺), and the number of Merkel complexes, visualized via TROMA-I antibody, were counted. Then, the length of the surface of the skin was traced and measured in ImageJ and multiplied by the thickness of the sections to obtain a volume in mm^3 . Density was calculated by dividing the number of corpuscles or Merkel complexes (clusters of Merkel cells) by the volume of skin.

Behavior

Mice used for behavioral experiments were kept on a reversed light-dark cycle and were tested during the dark phase. Male mice of mixed genetic background (C57BL/6J and CD1) were ear notched for identification and genotyped at approximately P21. Females were not used due to potential effects of the estrous cycle on behavior, and a preliminary observation that female mice have lower von Frey thresholds than male mice. Ear notching was performed using an ear punch device (Kent Scientific). Mice 6-16 weeks of age were subjected to behavioral tests.

Mutant animals were compared to control littermates from the same genetic crosses to control for strain/genetic background variability. All behavioral testing was performed by an experimenter blind to genotype.

Von Frey Paw Withdrawal Test

For the von Frey paw withdrawal test, a sheet of wire mesh (9217T52, McMaster-Carr) was attached to an acrylic frame and positioned about 14 inches above a table. Mice were placed in 5x2 inch clear, acrylic chambers, which were taped on top of the mesh. Prior to test date, mice were habituated to the chambers for one hour for two consecutive days. On the test date, withdrawal responses were measured. After allowing the mice to habituate for one hour, von Frey filaments (North Coast Medical) were applied to the left hindpaw. The experimenter applied the filament onto or within close proximity to the pedal pads of the hindpaw. Care was taken to avoid the hairy skin in the middle of the hindpaw. Starting with the lowest force, each filament was applied five times in a row, followed by a brief break. Then, the filament was applied another five times for a total of ten applications. The number of paw withdrawals was recorded for each filament weight.

Operant Conditioning Surgery and Water Restriction

Prior to operant conditioning, control *TrkB^{flox/flox}* and mutant *TrkB^{CKO}* mice were implanted with headplates to in order to restrain them to the operant conditioning behavior apparatus. Adult (>P60) mice were anaesthetized with isoflurane (1.75 - 2% in O₂). Following removal of the scalp and periosteum, MetaBond dental cement was used to secure a lightweight, titanium headplate to the skull. Five days after surgery, mice began water-restriction (40 ml/kg of initial body weight) until they weighed 85% of their pre-restriction weight. Animals were monitored for health conditions every training and testing day using a detailed health assessment adapted for water deprived mice (39). Health categories included weight, posture and grooming, activity level, signs of normal eating/waste elimination, and signs of dehydration. The minimum

required daily water intake for each animal was 0.8mL during data collection. Any animal that did not receive this much during the assay was supplemented up to the minimum volume.

Operant Conditioning Training

Mice were kept on a reversed light/dark cycle, and behavioral sessions were held daily for each animal. Behavioral paradigm control was performed by a custom written program running within the WaveSurfer application (Howard Hughes Medical Institute) in MATLAB. On the first and second days of training, each animal was given approximately one minute to freely roam the apparatus platform. Mice were then habituated to head restraint for 5-15 minutes with *ad libitum* water from the spout. To minimize the stress and movement of the animal, a three-sided acrylic enclosure was placed over the animal's body. On the third day of training, the right forepaw of each animal was secured over a 3-mm square hole in the apparatus platform, using an elastic strap over the forearm and clear cellophane tape over the back of the forepaw. A fine mechanical stimulator (Model 300 C-I, Aurora Scientific) positioned beneath the platform was used to apply a 75-mN step indentation stimulus to the glabrous skin of the forepaw. This indentation was applied atop a minimal force (< 1 mN) used to hold the arm in position. If the animal licked the spout within 2 s of the stimulus onset, it received a 5- μ l water reward. Over the next two weeks of training, the response period was reduced to 0.5 s, and a no-lick window of 3 s was introduced to discourage spurious licks. In the final phase of training, animals were presented with a range of stimulus amplitudes between 0.5 and 50 mN on 60% of trials, with 20% of all trials serving as no-stimulus (catch) trials, and 20% with a salient 75 mN stimulus to maintain task engagement. Within three weeks, animals exhibited stable psychometric

functions, with average response rate of $80.5 \pm 3.5\%$ and false alarm rate of $17.1 \pm 2.5\%$ (mean \pm s.e.m.) for the two days preceding data collection. Mice displayed some differences in overall sensitivity between von Frey and operant conditioning. Differences in stimulus application – including probe diameter, stimulus waveform, and holding force – likely account for these sensitivity differences.

Operant Conditioning Data Collection and Sorting

For all animals, data was collected for six days, following a pattern of two days of testing blocks followed by one day of an easier training paradigm. To exclude data when animals were not engaged in the behavior task, blocks of trials characterized by overall poor performance were omitted from analysis of the detection threshold. We used a d' statistic to identify these blocks of disengagement in the task, calculated using only trials with salient stimuli levels greater than 40 mN (equation 1).

$$d' = Z(\text{hit rate}) - Z(\text{false alarm rate}) \quad (1)$$

For the first and last 14 trials in a session, d' was calculated over the entire block and the same value was assigned to each of the 14 trials. For all other trials in a session, d' was calculated over blocks of 30 trials and the value was assigned to the middle trial in the block (i.e. the d' value for trial 15 was found using all stimulus trials over 40 mN between trials 1 and 30). Only blocks with at least 15 trials of d' greater than or equal to 1.5 were used in data analysis.

Animals with fewer than 750 viable trials were excluded.

To fit psychometric curves to the aggregate data, all stimulus trials were distributed into bins at 3 mN intervals, with the exception of the final bin with the most salient stimulus of 75 mN. For each animal, the average response rate during trials within each bin was calculated and averaged across all animals in either the control or *TrkB^{CKO}* group. The MATLAB software package ‘psignifit 4’ was used to fit a beta-binomial logistic sigmoid curve to each group (equation 2). Psignifit also output a parameter η that scaled the extra variance introduced within the bins of the data, where values near 1 indicated over-dispersed data and values near 0 indicated good binomial dispersion.

$$\psi(x; m, w, \lambda, \gamma) = \gamma + (1 - \lambda - \gamma) (1 + e^{-2 \log(1.05 - 1) x - mw}) \quad (2)$$

where x is binned stimulus intensity, m is the midpoint of the psychometric function, w is the width of the curve, λ is the upper asymptote, and γ is the lower asymptote. Average psychometric threshold for each group was determined by fitting individual mouse response data to a beta-binomial logistic sigmoid curve using Psignifit. For each mouse, the force value at the midpoint of the psychometric function was determined to be its psychometric threshold. This data was then averaged within group.

Horizontal Ladder Assay

For the horizontal ladder assay, a ladder consisting of two parallel acrylic sheets as sides and equally spaced aluminum rods was mounted above a table. An angled mirror was positioned

below the ladder to increase visibility of foot position. The lighting in the testing room was dim to eliminate visual input as much as possible. Mice were trained on the ladder during two consecutive habituation days. During habituation, mice were placed on one end of the ladder and were allowed to walk across the ladder towards a cage on the opposite end. Trials in which the mice paused for more than five s, turned around, or walked on the rim of the ladder rather than the rungs were immediately repeated. This continued until mice successfully crossed the ladder three times, but each mouse was subjected to no more than five total trials per day. On the third day, videos of the mice crossing the ladder were recorded, and the number of slips and time to cross the ladder were measured by an experimenter who was blinded to genotype. The average values of three successful trials were obtained for each animal.

Wire Hang Assay

For the wire hang assay, a 35 cm aluminum wire (~2.5 mm in diameter) was hung about 14 inches above a table using two aluminum columns attached to a base. Two paper plates were positioned on each end of the wire to prevent mice from moving to the columns. The mouse was placed in the center of the wire, and a cage with bedding was placed below the mouse to provide a cushioned landing area. For each mouse, the time from placement on the wire to falling was measured for three successful trials. Mice that remained on the wire for 90 s or longer were removed from the wire, and their time to fall was counted as 90 s. Additionally, trials in which mice fell instantly after placement on the wire were not counted as successful, and the trial was repeated.

Tactile Prepulse Inhibition (PPI) assay

Control and *TrkB^{CKO}* Mice were subjected to the tactile inhibition assay, a measure of hairy skin sensitivity, as described(40).

Sunflower seed handling measurements

Sunflower seed habituation in home cages: One week prior to testing animals were habituated to black oil sunflower seeds, Bio-Serv, S5137-1, Wagner's, 76025, in their home cage by adding one to two tablespoons of seeds to the floor of the cage for five consecutive days. If animals did not recognize seeds as a food source a teaspoon of seeds were cracked before adding to the cage floor.

Behavior chamber habituation and handling two days prior to sunflower seed testing: Animals were habituated to behavior room environment and investigator handling by undergoing tail inking on habituation day 1. To ink the tail, each animal was gently lifted and placed on the cage wire food hopper facing away from investigator. Firmly holding the tail midway from the tail base, a blue permanent soy ink marker was rolled across the tail forming parallel lines to indicate identifying ear notch number. Once inked animals were gently transferred back into the home cage to await test chamber habituation.

The test chamber was constructed of a black matte acrylic wall and three optically clear walls, 10in(l) x 8in(w) x 8in(h), 0.25 in thick, centered on a white matte acrylic floor under diffuse warm white light (2700K). Three digital USB 2.0 CMOS video cameras mounted on camera

sliders were positioned on each clear side of the test chambers. One additional overview camera was mounted directly above the test chamber.

Assay and behavioral measurements: Seeds were withheld from the home cage for two days prior to and during testing to encourage foraging and seed eating in the test chamber. During habituation day 1 and day 2, animals were removed from the home cage and placed in an empty test chamber resting on the white matte acrylic floor. Each animal was given 2-3 seeds while freely exploring the test chamber for 20 minutes. Following the free exploration period animals were returned to their home cages. On testing day 3, animals were transferred from their home cage and placed in the test chamber and allowed to explore the chamber for 5 minutes. Following acclimation, 2-3 seeds were placed on the floor of the test chamber and the seed eating activity was recorded. At the completion of the test, animals were removed from the test chamber and returned to their home cage. Chambers were reset and cleaned with unscented soapy water, wiped down with distilled water, and dried. Animals that failed to eat seeds after 20 minutes were returned to their home cage and the test was rescheduled. This approach was repeated until each animal fully deshelled and consumed multiple seeds. Seeds that were partially shelled, partially consumed, or discarded were not counted. Behaviors were measured by defined seed deshelling/eating actions: 1. Seed peeling/deshelling – the act of grasping/holding the sunflower seed between the forepaws, clamping the upper and lower incisors into the shell surface and applying downward force (dip) that pushed the shell away from the head/teeth towards the floor. This action resulted in a systematic peeling of the shell to expose the seed kernel. Animals unable to maintain a firm grip on or fully grasp the shell

would typically adapt by touching, tapping, resting and/or bracing the seed against the floor between the forepaws. Animals also “tucked” the shell against their abdomen, holding the shell between the forepaws, clamping their upper and lower incisors onto the shell surface pulling their heads backwards away from the shell/forepaws to peel off sections of the shell exposing the seed kernel. 2. Touch/Taps - the act of touching and/or holding and/or bracing the seed shell between the forepaws and the floor during seed peeling. 3. Dip – the act of holding the seed shell between forepaws, clamping shell between incisors and applying downward force to peel off sections of shell. 4. Rotate – the act of or ability to change and/or manipulate shell orientation within the forepaws. 5. Rocking – the act of grasping the shell between the forepaws with shell firmly between incisors, using forepaws to “rock” shell side-to-side between incisors to bite into the shell to peel and expose the seed kernel.

RESOURCES TABLE for Sunflower seed assay

REAGENT or RESOURCE	SOURCE	IDENTIFIER
GRAPHPAD Prism 8	GraphPad Software 7825 Fay Avenue, Suite 230 La Jolla, CA 92037 USA Phone: 858-454-5577 Fax: 858-454-4150 sales@graphpad.com support@graphpad.com	
IC Capture Video Acquisition Software	The Imaging Source, LLC Suite 400 6926 Shannon Willow Rd Charlotte, NC 28226 United States Phone: 704-370-0110 https://www.theimagesource.com/	
Stoelting Digital USB 2.0 CMOS Camera	Stoelting Co. 620 Wheat Lane, Wood Dale, IL 60191	Camera: 60516 Vari-focal, 2.8-12mm

	T: 630.860.9700 F: 630.860.9775 E: info@stoeltingco.com www.stoeltingco.com	Lens: 60528
Bio-Serv Black Oil Sunflower Seeds	Bio-Serv 3 Foster Lane Flemington, NJ 08822 US Phone: 800-996-9908 https://www.bio-serv.com/	S5137-1
Wagner's Four Season Oil Sunflower Seed	Wagner's, LLC P.O. Box 54 Jericho, N.Y. 11753 Phone: 516-933-6580 Fax: 516-933-6581 info@wagners.com	76025
Sunflower Seed Test Chamber Black Matte, Optically Clear Acrylic 0.25in, 10in(l) x 8in(w) x 8in(h)	Altec Plastics Inc. 116 B Street South Boston, MA 02127 617.269.1400 info@altecplastics.com https://shop.altecplastics.com/	
Sunflower Seed Floor, White Matte Acrylic 0.25in 36in(l) x 26in(w)	Altec Plastics Inc. 116 B Street South Boston, MA 02127 617.269.1400 info@altecplastics.com https://shop.altecplastics.com/	

Gait analysis

A recording setup based on a modified design of LocoMouse (41) was built for high speed, automated analysis of mouse locomotion behavior. The dimensions of the transparent corridor used were 64.5 (L) x 4 (W) x 6 (H) cm. Dark enclosures were situated on both ends of the corridor and the animal freely moved between the two ends. Acquisition were triggered by

infrared sensors during each epoch of corridor crossing. Two mirrors angled at 48 degrees downward flanked the longitudinal axis of the corridor, which projected the side views of the animal to a camera below. A single high-speed camera (Bonito CL-400B/C 2320 x 700 pixels, Allied Vision, Exton, PA.) captured simultaneous videos of the bottom view and two side views of the animal at 200 fps. Videos of the animal were compressed and analyzed offline using a convolutional neural network for postural tracking written in PyTorch and MATLAB (Mathworks, Natick, MA). Briefly, an hourglass network based on Ref. (42) was trained on 1000 expert annotated frames to simultaneously recognize the following body parts in the bottom and side views: nose, start and end of the tail, forepaws and hind paws. The positions of body parts from all three perspectives were combined to generate a three-dimensional postural time series. A hidden Markov model was used to infer the start and the end of each gait cycle based on paw velocity. The following parameters are measured for each gait cycle: velocity, height, tail elevation, hind paw width, cadence, stride length, paw width, stand duration, vertical and horizontal tail oscillation. A linear mixed effect model of the form $Y \sim \text{Intercept} + \text{Genotype} + \text{Sex} + \text{Genotype}:\text{Sex} + (1 | \text{Name})$ and ANOVA was used for statistical testing. In the case where velocity is considered as an independent variable, a model of the form $Y \sim \text{Intercept} + \text{Velocity} + \text{Genotype} + \text{Sex} + \text{Genotype}:\text{Sex} + \text{Velocity}:\text{Genotype} + \text{Velocity}:\text{Sex} + (1 | \text{Name})$ was used instead.

Electron Microscopy

Forepaw toe pads (ages P21-P39) were excised and immersed in a glutaraldehyde/formaldehyde fixative for 1 hour at room temperature, further dissected, and

subsequently fixed overnight at 4 °C. Sample preparation was done as previously described (28). Ultrathin sections were cut at 40-60 nm and imaged using a JEOL 1200EX transmission electron microscope at 80 kV accelerating voltage. Images were cropped and adjusted with normalization to enhance contrast using Fiji/ImageJ. For corpuscles that were larger than the imaging field, montage of images was generated using TrakEM2 (43). Only sections close to the center of Meissner corpuscles were included for quantification. Axons that did not have apparent lamellar wrappings were not included. Two researchers, not involved in EM data collection and blind to genotypes, independently counted the number of lamellar wrappings around designated axons. The counts from both researchers were averaged for final analysis. Differences in lamellar wrapping counts per axon between these two researchers ranged from 0 to 5 wrappings.

Modeling

To find the mutual information between point stimulus location and neural population response, we assumed K possible point stimulus locations, denoted s , where each of them is equally likely to occur, that is, $p(s) = 1/K$ for all s . Furthermore, we assumed $M (\leq K)$ distinct neural population responses, denoted r , where response $r = m$ corresponds to n_m different point stimulus locations. Some locations might not have tactile receptors, such that $L = \sum_{m=1}^M n_m \leq K$. Overall, the set $\{n_1, \dots, n_M\}$ determines the efficiency with which neural population responses encode tactile location.

To find the mutual information between point stimulus location s and neural population response r , we use $\text{MI}(s; r) = H(s) - H(s|r)$, where $H(s)$ is the entropy of stimulus locations, and $H(s|r)$ is the conditional entropy, conditioned on a particular population response. Due to the uniform stimulus location distribution, we have $H(s) = \log_2 K$. To find the conditional entropy, we observe that $p(s|r = m) = 1/n_m$ for all locations s that yield population response $r = m$, and $p(s|r = m) = 0$ otherwise. This results in

$$H(s|r) = - \sum_s p(s) \sum_{m=1}^M p(s|r = m) \log_2 p(s|r = m) = - \sum_{m=1}^M \frac{n_m}{K} \log_2 \frac{1}{n_m},$$

where we have used the fact that each stimulus location corresponds to at most one population response. Overall, this yields the mutual information:

$$\text{MI}(s; r) = \log_2 K + \sum_{m=1}^M \frac{n_m}{K} \log_2 \frac{1}{n_m}.$$

In this expression, n_m/K is the overall fraction of stimulus locations that evoke population response $r = m$, and $1/n_m$ is the probability of each stimulus location given this response.

To find the set $\{n_1, \dots, n_M\}$ that maximizes the mutual information, we define the column vector $\vec{n} = (n_1, \dots, n_M)^T$ and write the mutual information in vector form, $\text{MI}(s; r) = \log_2 K + K^{-1} \vec{n}^T \log_2 1/\vec{n}$, where the last division is element-wise. We can then perform a constraint optimization on \vec{n} with constraint $\vec{1}^T \vec{n} = L$, resulting in $n_m^* = L/M$ for all m . Thus, optimal

coding (under the above assumptions) distributes the population responses evenly across stimulus locations. Furthermore, the mutual information increases with L , such that it is maximized if all stimulus locations yield a neural response (i.e., there are no gaps in the receptive fields), when $L^* = K$. Under these circumstances, the mutual information becomes $MI(s; r) = \log_2 M$, providing an upper bound.

For non-overlapped, square receptive fields, the number of distinct population responses M equals the number of neurons N . If these receptive fields tile the whole stimulus space evenly, then the associated mutual information is $MI(s; r) = \log_2 N$. As the number of discriminable spaces is $2^{MI(s; r)} = N$, the number of efficiently discriminable spaces per neuron is $2^{MI(s; r)}/N = 1$.

For overlapped, square receptive fields, each stimulus location within the receptive field of two distinct neurons results in a distinct neural population response. Two non-overlapped layers with $N/2$ equally sized square receptive fields that are offset against each other result in $4(N/2) = 2N$ distinct population responses (ignoring boundary effects, which become negligible for large N). These responses evenly tile the stimulus space if the offset is maximized, in which case $MI(s; r) = \log_2 2N$. This results the number of efficiently discriminable space per neuron to be given by $2^{MI(s; r)}/N = 2$.

The two-point discrimination capability of square receptive fields was modeled by imagining a point stimulus presented to the center of a discriminable space and a circle of points presented

at some distance d from the central point. The central point and the shifted point were presented asynchronously. For a given d , the fraction of the circle's circumference that extended outside the central discriminable space into a new discriminable space was considered the percent correct (i.e. the percentage of points unambiguously distinguishable from the central point). For non-overlapped squares with side length s and with a central point presented within a single square:

$$\% \text{ correct} = \begin{cases} 0, & d \leq \frac{s}{2} \\ 100 \frac{4}{\pi} \cos^{-1} \frac{s}{2d}, & \frac{s}{2} < d \leq \frac{s}{\sqrt{2}} \\ 100, & d < \frac{s}{\sqrt{2}} \end{cases}$$

For overlapped squares with side length $\sqrt{2}s$ and with a central point presented within a discriminable space:

$$\% \text{ correct} = \begin{cases} 0, & d \leq \frac{s}{2\sqrt{2}} \\ 100 \frac{4}{\pi} \cos^{-1} \frac{s}{2\sqrt{2}d}, & \frac{s}{2\sqrt{2}} < d \leq \frac{s}{2} \\ 100, & d < \frac{s}{2} \end{cases}$$

To model irregular and variable receptive fields, images of overlapped and non-overlapped Voronoi tessellations were generated in MATLAB using the voronoi function. The image set consisted of 4000 tessellations seeded with 84-101 random points in a square window. Number of neurons, N , for a single tessellation was the number of seeded points forming Voronoi cells that were within the window. Pairs of tessellations were overlapped to create 2000 overlapped mosaics with number of neurons equal to the combined number of neurons in the overlaid pairs. Mutual information between neural responses r and stimuli s was defined as above:

$$MI(s; r) = H(s) - H(s|r) = \log_2 K + \sum_{m=1}^M \frac{n_m}{K} \log_2 \frac{1}{n_m}$$

where K is the total number of pixels and n_m are the number of pixels per discriminable space. Mutual information was normalized by the number of neurons ($2^M/N$). The difference between overlapped and non-overlapped Voronoi tessellations was determined to be statistically significant using 5000 bootstrap samples, each consisting of a randomly chosen pair from the 2000 overlapped tessellations and 2000 non-overlapped tessellations.

Code Availability

The computer code that supports the findings of this study is available from the corresponding author upon reasonable request.

Data Availability

The data that support the findings of this study are available from the corresponding author upon reasonable request.

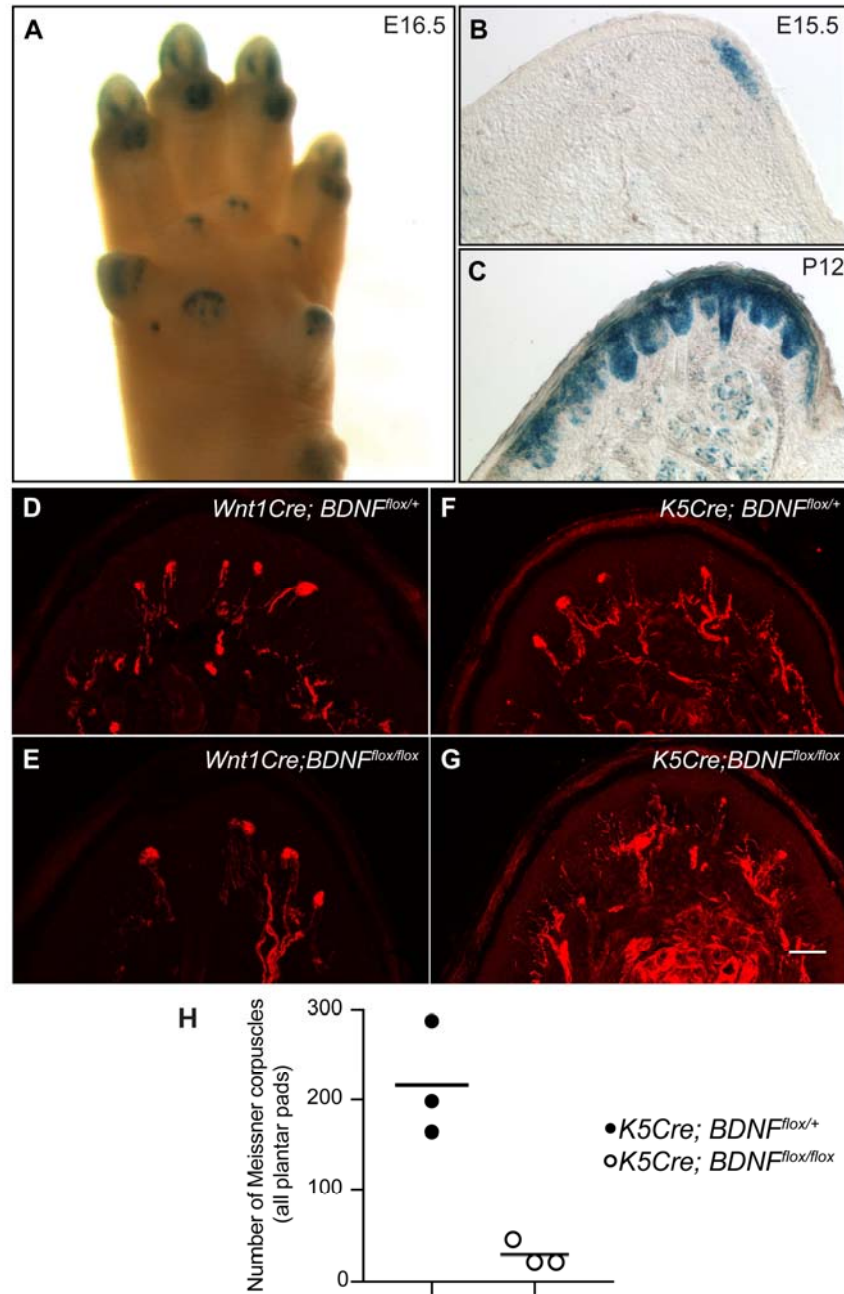


Fig. S1. BDNF expressed in epithelial cells, but not in neural crest-derived sensory neurons or Schwann cells, is essential for Meissner corpuscle formation.

A. Whole forelimb of an E16.5 $BDNF^{lacZ}$ embryo stained using X-gal.

B-C. Forelimb palmar pad sections of $BDNF^{lacZ}$ mice at E15.5 and P12 stained with X-gal.

D-G. Hindlimb plantar pad sections were stained with anti-S100 to reveal Meissner corpuscles

in *Wnt1Cre; BDNF^{flox/flox}* mice, in which BDNF expression is eliminated in DRG sensory neurons and Schwann cells, and control mice. The number of Meissner corpuscles in glabrous skin of control and *Wnt1Cre; BDNF^{flox/flox}* mice are comparable, and this comparison was done with two pairs of control (105 and 133 corpuscles in two hindlimb pedal pads per mouse) and *Wnt1Cre; BDNF^{flox/flox}* mice (119 and 89 corpuscles in two hindlimb pedal pads per mouse). (scale bar = 50 μm)

H. Quantifications of the number of Meissner corpuscles in all hindlimb plantar pads of *K5Cre; BDNF^{flox/flox}* mice, in which BDNF expression is eliminated in skin epithelial cells, and control mice at P20 (3 mice for each genotype, 6 hindlimb pedal pads per mouse). Black bars represent means. Serial sections were cut throughout the whole plantar region and Meissner corpuscles were identified by S100 staining and counted across all sections.

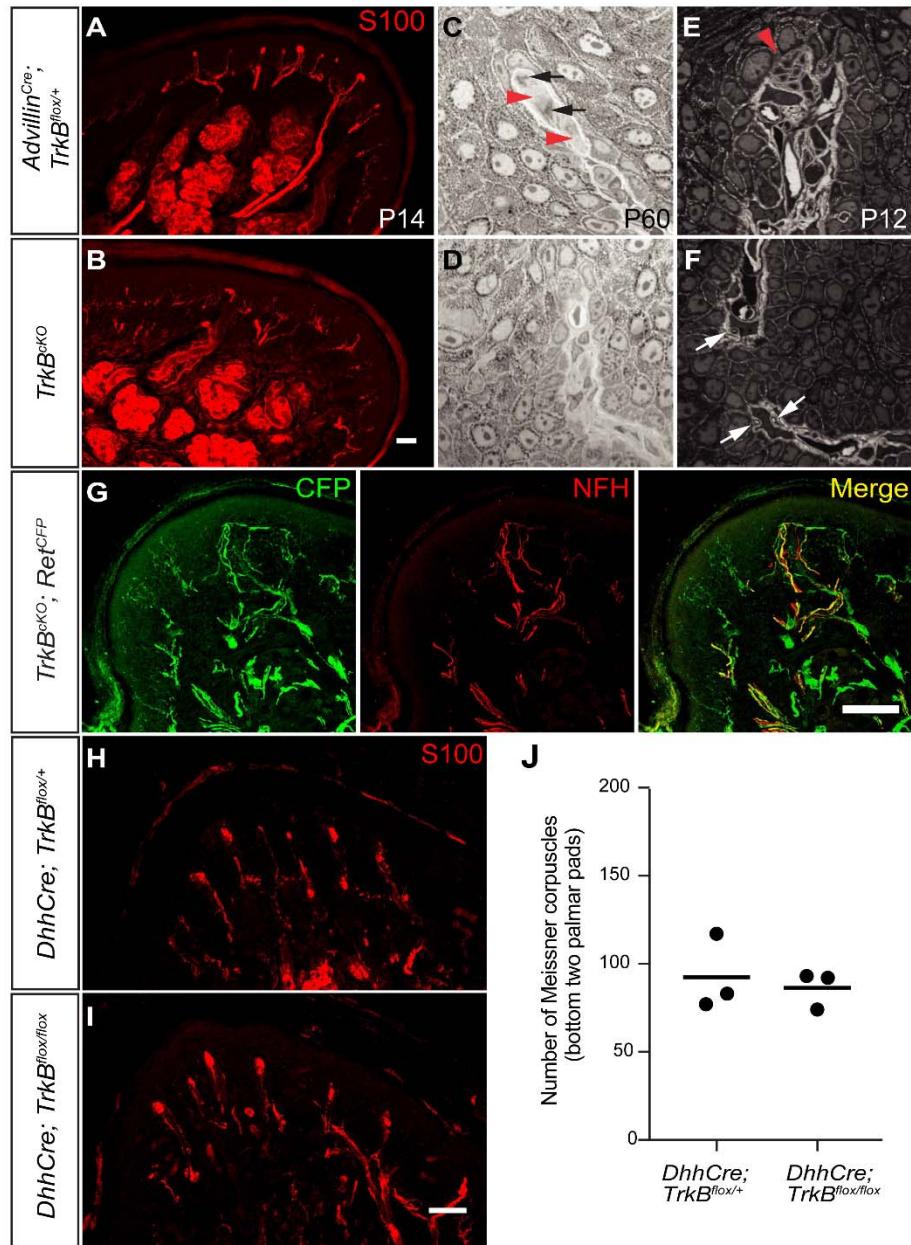


Fig. S2. TrkB is required in sensory neurons, but not glia cells, for the formation of Meissner corpuscles and their innervating sensory neurons.

A-B. Hindlimb plantar pad sections of control and *TrkB^{CKO}* mice at P14 stained with anti-S100 antibody. (scale bar = 50 μ m)

C-F. To exclude the possibility that in sensory-neuron-specific *TrkB^{CKO}* mice Meissner corpuscles

are formed but fail to express S100 protein, we performed toluidine/methylene blue staining on semi-thin sections of the glabrous skin. Semi-thin sections (0.5 μm) of hindlimb plantar pads of control and *TrkB^{CKO}* mice were cut parallel to the skin surface. In C and D, mice were sacrificed at P60, and staining was done with methylene blue. Red arrowheads: cytoplasmic processes of lamellar cells; black arrows: nerve terminals (densely stained). In E and F, mice were sacrificed at P12, and staining was performed with toluidine blue. Red arrowheads: premature corpuscle, white arrows: large caliber nerve fibers. No Schwann cells were observed in the dermal papillae of adult or P12 *TrkB^{CKO}* mice. These experiments were performed in 2 animals per age with similar results.

G. A forelimb palmar pad section of a P14 *TrkB^{CKO}; Ret^{CFP}* mouse stained with anti-GFP and anti-NFH antibodies. The majority of the NFH⁺ fibers present in glabrous skin dermal papillae at P14 are CFP⁺. This experiment was performed in 2 mice with similar results. (scale bar = 50 μm)

H-I. Hindlimb plantar pad sections of control and *DhhCre; TrkB^{flox/flox}* mice at P20 stained with anti-S100 antibody. *DhhCre* mice express Cre recombinase in all Schwann cells. (scale bar = 50 μm)

J. Quantification of the number of Meissner corpuscles in control and *DhhCre; TrkB^{flox/flox}* mice at P20. Meissner corpuscles in the bottom two palmar pads of each forelimb were counted (3 mice for each genotype). Black bars represent means.

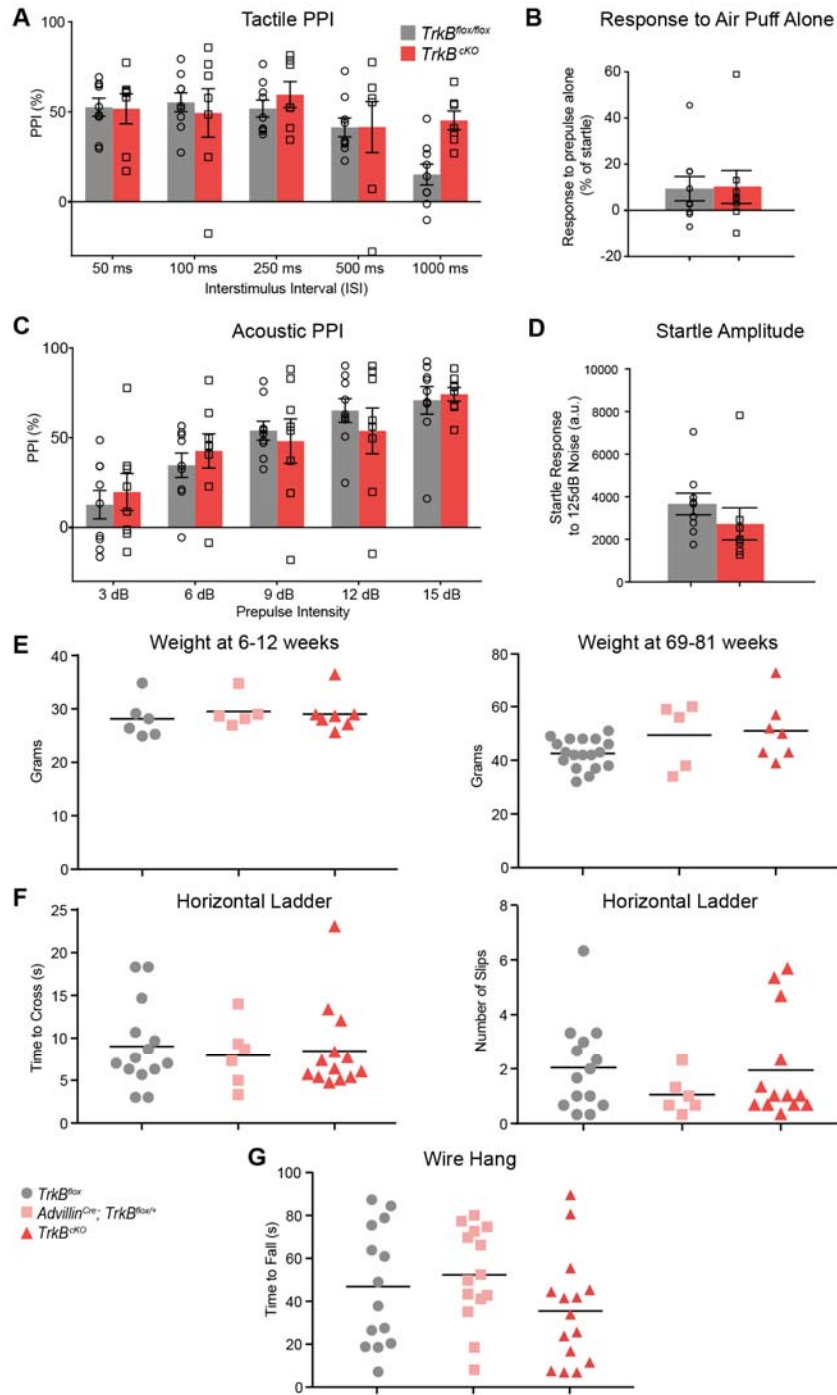


Fig. S3. *TrkB^{cko}* mice have normal hairy skin sensitivity and are overtly normal.

A. Percent inhibition of the startle response to a 125-dB noise (pulse), when the startle noise was preceded by a light air puff (prepulse, 0.9 PSI, 50 ms) applied to the back hairy skin at

multiple inter-stimulus intervals (ISIs) between the prepulse and the pulse, for *TrkB^{CKO}* mutant mice and control littermates. Repeated measures, two-way ANOVA: no significant differences between genotypes.

B. Response to a light air puff (0.9 PSI, 50 ms) applied to the back hairy skin, for *TrkB^{CKO}* mutant mice and control littermates. Responses are expressed as a percent of startle response to a 125-dB noise. Student's t-test, not significant. N= 9 (control littermates) and 8 (*TrkB^{CKO}* mutants).

C. Percent inhibition of the startle response to a 125-dB noise (pulse), when the startle noise is preceded by a non-startling tone prepulse (80 dB for 20 ms, with a 100 ms ISI) in *TrkB^{CKO}* mutant mice and control littermates. Repeated measures, two-way ANOVA: no significant differences between genotypes.

D. Magnitude of startle response to a 125-dB noise in *TrkB^{CKO}* mutant mice and control littermates. Student's t-test, not significant.

E. Left: Weights of adult (6-12 weeks old) male control and *TrkB^{CKO}* mice are similar. Right: Weights of aged adult (69-81 weeks old) control and *TrkB^{CKO}* mice are also similar. Black bars represent means.

F *TrkB^{CKO}* mice performed similarly to controls when crossing a horizontal ladder. Each point represents the average of three trials for each animal, and black bars represent means.

G. *TrkB^{CKO}* mice performed similarly to controls when hanging from a suspended wire. Each point represents the average of three trials for each animal, and black bars represent means.

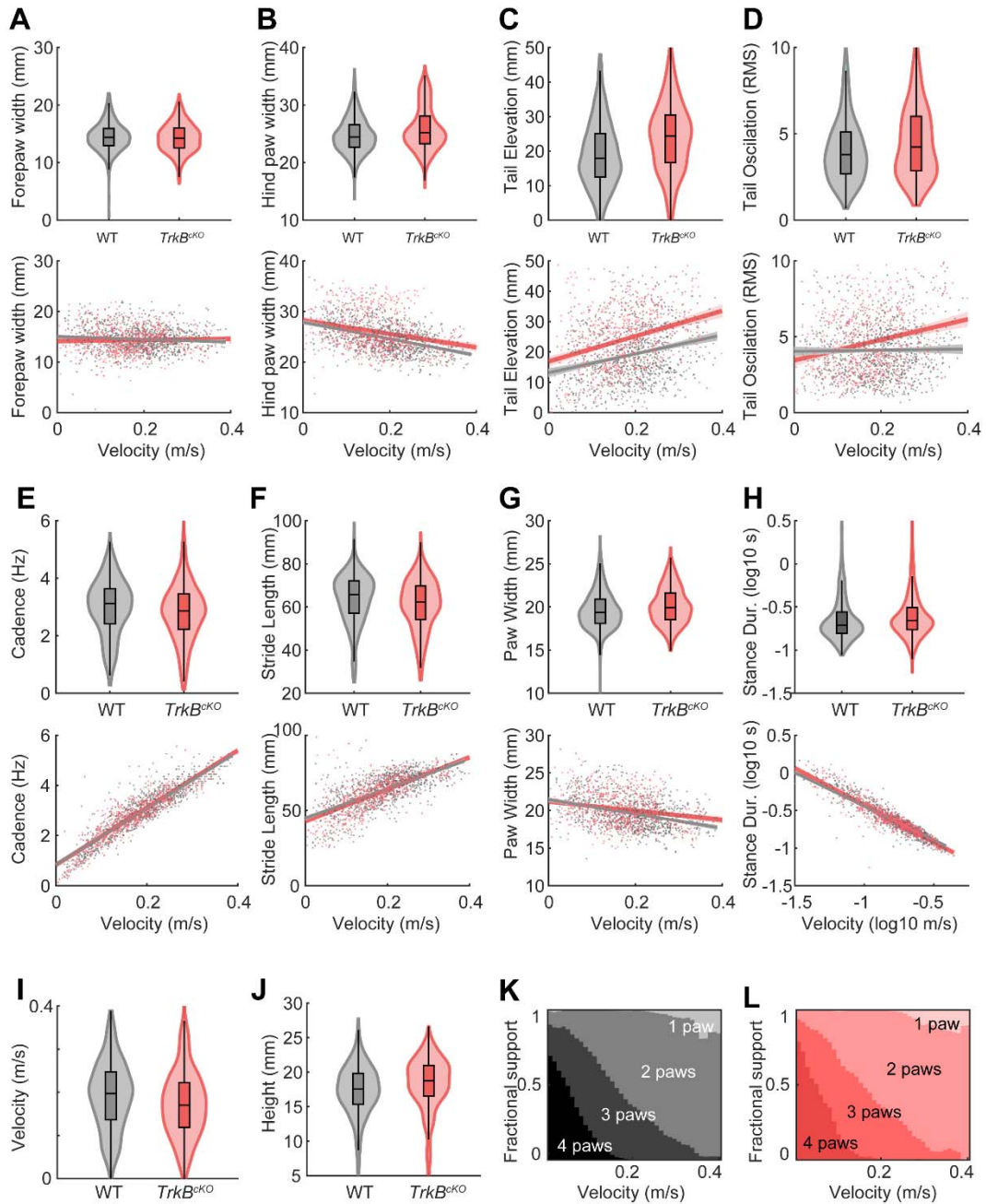


Fig. S4. *TrkB^{CKO}* mice have normal gait but more tail oscillation is observed at higher velocity.

A-H. Violin plots (top) and regression analyses with velocity as an independent variable (bottom) for animal forepaw width (A), hindpaw width (B), tail elevation (C), tail oscillation (D), cadence (E), stride length (F), paw width (contralateral forepaw to hindpaw) (G), average stance duration (H) for control mice in grey and *TrkB^{CKO}* mice in red.

I-J. Violin plots for velocity (I) and height (J)

K-L. Fraction of time during a single gait cycle for a given velocity when the subject had four (darkest) to one (lightest) paws on the floor for support. Control mice in grey and *TrkB^{CKO}* mice in red.

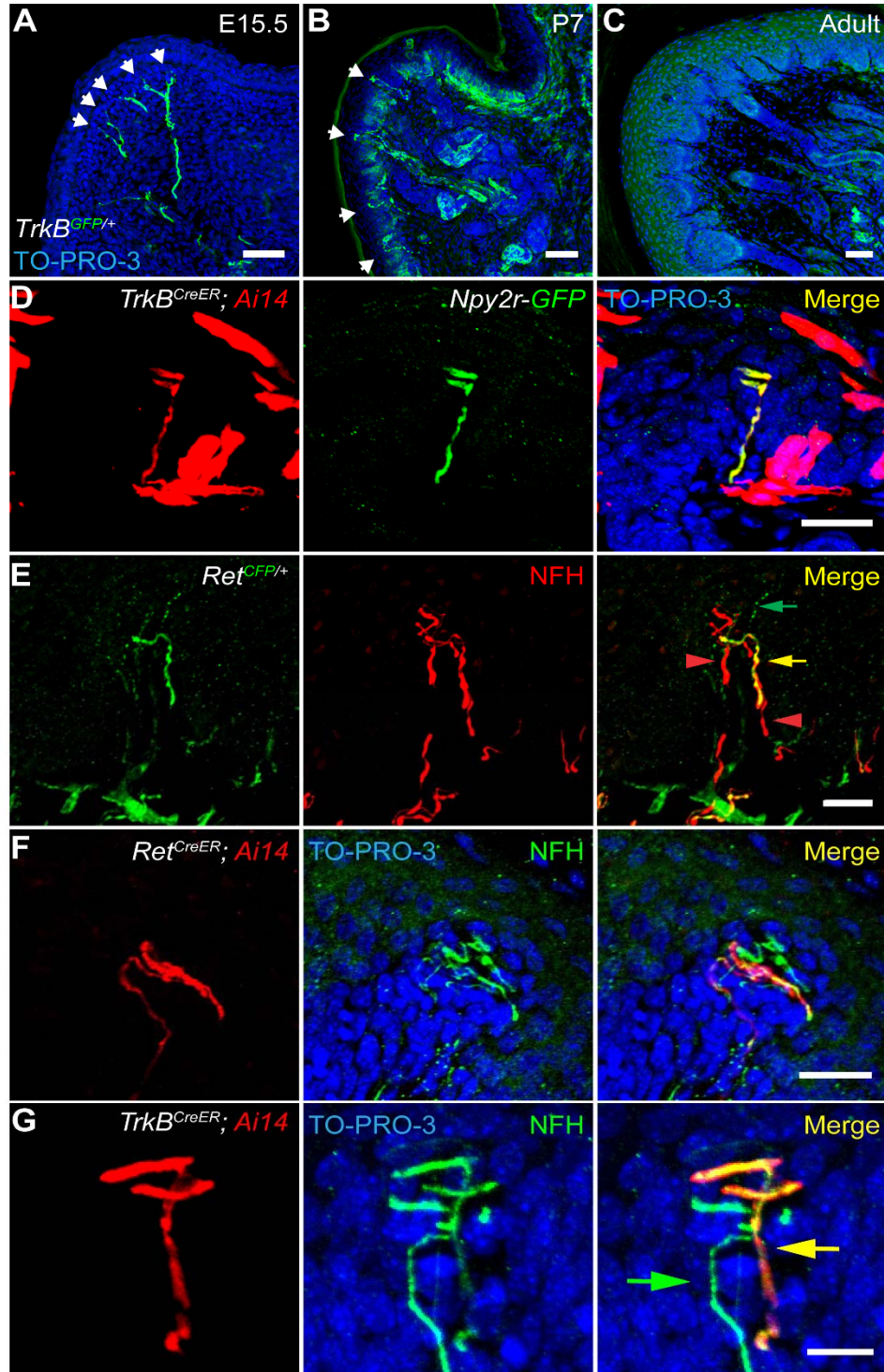


Fig. S5. *TrkB*⁺ and *Ret*⁺ neurons innervating Meissner corpuscles are distinct populations of neurofilament-positive afferents.

A-C. Forelimb palmar pad sections of *TrkB^{GFP}* mice at different developmental stages stained

with anti-GFP and TO-PRO-3. Note that GFP is expressed in Meissner corpuscle afferents at an early age (P7), but not in adults. These experiments were performed in multiple animals with similar results (A: 2 mice, B: 4 mice, C: 2 mice). (scale bar = 50 μ m)

D. Glabrous skin section of a P20 *TrkB^{CreER}; Ai14; Npy2r-GFP* mouse treated with tamoxifen at P5 to permanently label early *TrkB⁺* neurons. Section was stained with anti-DsRed, anti-GFP, and TO-PRO-3. Result observed in 6 corpuscles of 1 mouse. (scale bar = 25 μ m)

E. A hindlimb digital pad section of a P50 *Ret^{CFP}* mouse stained with anti-GFP and anti-NFH antibodies. This experiment was performed in 3 mice with similar results. Yellow arrow: *CFP⁺/NFH⁺* Ret fiber. Green arrow: *CFP⁺/NFH⁻* nonpeptidergic C-fiber. Red arrowheads: *NFH⁺/CFP⁻* fibers. (scale bar = 25 μ m)

F. Forelimb pedal pad section of a P20 *Ret^{CreER}; Ai14* mouse treated with tamoxifen at E10.5-E11.5. Section was stained with anti-NFH antibody and TO-PRO-3. This experiment was performed in 2 mice with similar results. (scale bar = 25 μ m)

G. A hindlimb digital pad section of a P50 *TrkB^{CreER}; Ai14* mouse treated with tamoxifen at E16.5 (same mouse as used in Figure 3B). Section was stained with anti-DsRed, anti-NFH, and TO-PRO-3. This experiment was performed in 3 mice with similar results. (scale bar = 12.5 μ m).

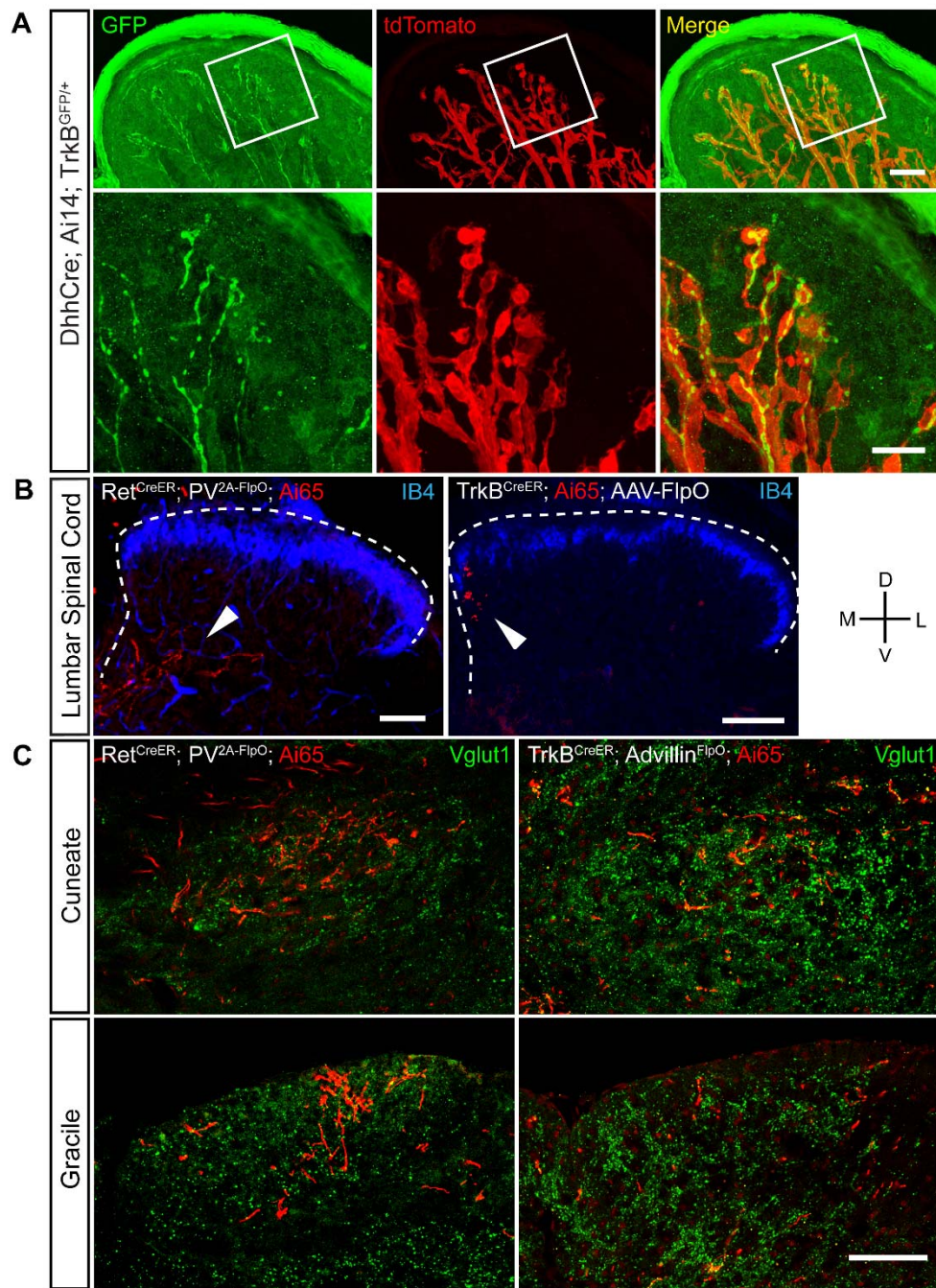


Fig. S6. Schwann cells are associated with TrkB-expressing fibers in dermal papillae during development and both TrkB⁺ and Ret⁺ Meissner corpuscle afferents form projections in the spinal cord and DCN.

A. Upper panels: A forelimb palmar pad section of a P5 *DhhCre; TrkB^{GFP}; Ai14* mouse stained with anti-GFP antibody. Schwann cells have not yet differentiated into lamellar cells at this age. TdTomato, which is expressed in Schwann cells, was detected via direct fluorescence. For each GFP⁺ fiber in dermal papillae, there are Schwann cell(s) associated with its tip. Lower panels: enlarged views of the region cropped in upper panels. This experiment was performed in 3 mice with similar results. (scale bars = 50 μm)

B. Transverse sections of lumbar spinal cords. Left panel is from a P21 *Ret^{CreER}; PV^{2A-FlpO}; Rosa26^{LSL-FSF-tdTomato} (Ai65)* mouse treated with tamoxifen at E11.5 and E12.5 (similar results were observed in three mice), and right panel is from an adult *TrkB^{CreER}; Ai65* mouse treated with tamoxifen at P5 and given an injection of AAV-FlpO to a glabrous hindlimb pedal pad to achieve labeling of a single TrkB⁺ Meissner afferent (a second section from this animal and sections from the other three animals are in Figure S6). Both sections were stained with anti-DsRed antibody and IB4. Arrowheads indicate dorsal horn collaterals. (scale bars = 100 μm, D = dorsal, V = ventral, M = medial, L = lateral)

C. Transverse sections of the medulla at the level of the cuneate and gracile nuclei of the DCN. Left panels are from a P21 *Ret^{CreER}; PV^{2A-FlpO}; Ai65* mouse treated with tamoxifen at E11.5 and E12.5 (DCN innervation observed in 3/3 mice), and right panels are from a P23 *TrkB^{CreER}; Advillin^{FlpO}; Ai65* mouse treated with tamoxifen at E13.5 and E14.5 (DCN innervation observed in this mouse and another adult mouse given tamoxifen at P4). All sections were stained with anti-Vglut1 and anti-DsRed antibodies. (scale bar = 100 μm; D = dorsal, V = ventral, M = medial, L = lateral)

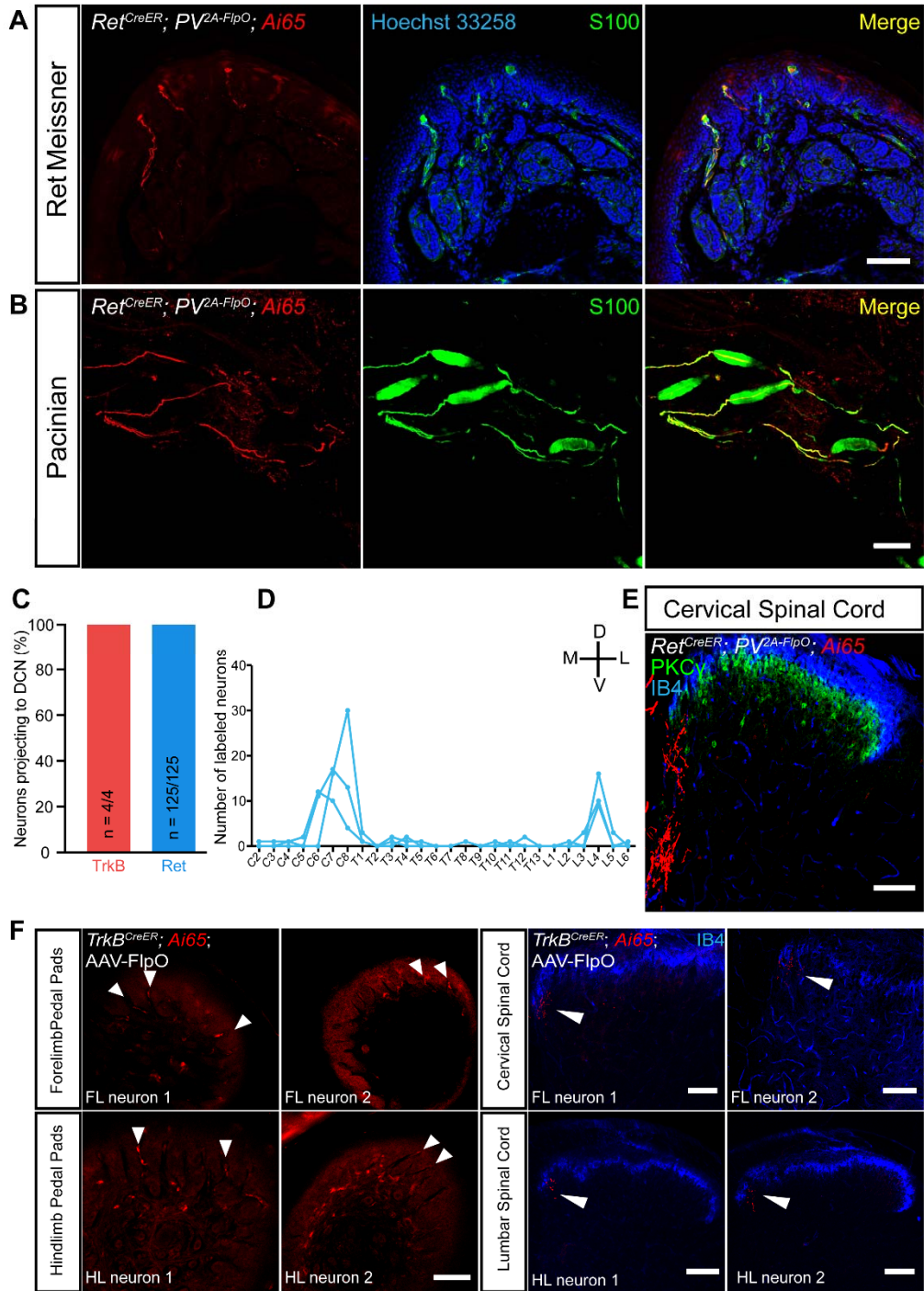


Fig. S7. *TrkB*⁺ and *Ret*⁺ Meissner corpuscle afferents display typical A β -LTMR morphology in the central nervous system.

A-B. A Ret-parvalbumin intersectional genetic strategy predominantly labels Ret⁺ neurons innervating Meissner and Pacinian corpuscles. No tdTomato⁺ neurons were observed in back and hindlimb hairy skin or in proprioceptors of the anterior tibialis muscle. A is a digital pad section from a P21 *Ret^{CreER}; PV^{2A-FlpO}; Ai65* mouse treated with tamoxifen at E11.5 and E12.5. Anti-S100 antibody labels Meissner corpuscles in the dermal papillae and Schwann cells surrounding the innervating sensory neurons. B is whole-mount immunostaining of Pacinian corpuscles located in the periosteum of the fibula from a *Ret^{CreER}; PV^{2A-FlpO}; Ai65* mouse. Anti-S100 antibody labels Pacinian corpuscles and Schwann cells surrounding the innervating sensory neurons. Skin sections and whole-mount Pacinian corpuscles were stained with anti-DsRed antibody. This experiment was performed in 3 mice with similar results. (scale bars = 100 μm).

C. Percentage of TrkB⁺ pedal pad Meissner neurons traveling to the DCN via the dorsal columns at the transition between cervical spinal levels and the medulla (4/4 neurons from 4 *TrkB^{CreER}; Ai65* mice with AAV-FlpO injection into the pedal pads, 2 hindlimb and 2 forelimb), and percentage of Ret⁺/PV⁺ neurons (Pacinian and Meissner afferents, see Figure S6) traveling to the DCN (number of neurons in the dorsal column at the medulla was compared to number of fluorescent neurons in the DRG, 2 *Ret^{CreER}; PV^{2A-FlpO}; Ai65* mice, 76/76 and 49/49 neurons labeled in the DRG, respectively). Note that the dual genetic/paw virus injection strategy has a low labeling efficiency and marks few neurons per animal.

D. Number of tdTomato⁺ neurons in the DRG per spinal segment in three *Ret^{CreERT2}; PV^{2A-FlpO}; Ai65* mice. This is consistent with the finding that the Ret-PV intersectional strategy

predominantly labels limb-level Pacinian afferents and Meissner afferents innervating glabrous skin.

E. Transverse section of cervical spinal cord from a P21 *Ret^{CreER}; PV^{2A-FlpO}; Ai65* mouse treated with tamoxifen at E11.5 and E12.5. Section was stained with anti-DsRed, anti-PKC γ , and IB4.

This experiment was performed in 3 mice with similar results. (scale bar = 100 μm ; D = dorsal, V = ventral, M = medial, L = lateral)

F. Peripheral terminations in the glabrous skin (arrowheads, left panels) and example spinal cord collateral morphologies (arrowheads, right panels) for single forelimb (FL) and hindlimb (HL) pedal pad neurons in adult *TrkB^{CreER}; Ai65* mice treated with tamoxifen at P5 and given an injection of AAV-FlpO to a glabrous pedal pad in order to achieve sparse labeling of a single neuron per animal. Whole-mount pedal pads were stained with anti-dsRed. Spinal cord sections were cut transversely and stained with IB4 and anti-dsRed. Another spinal cord section from HL neuron 1 is depicted in Figure S5. (scale bars = 100 μm ; D = dorsal, V = ventral, M = medial, L = lateral)

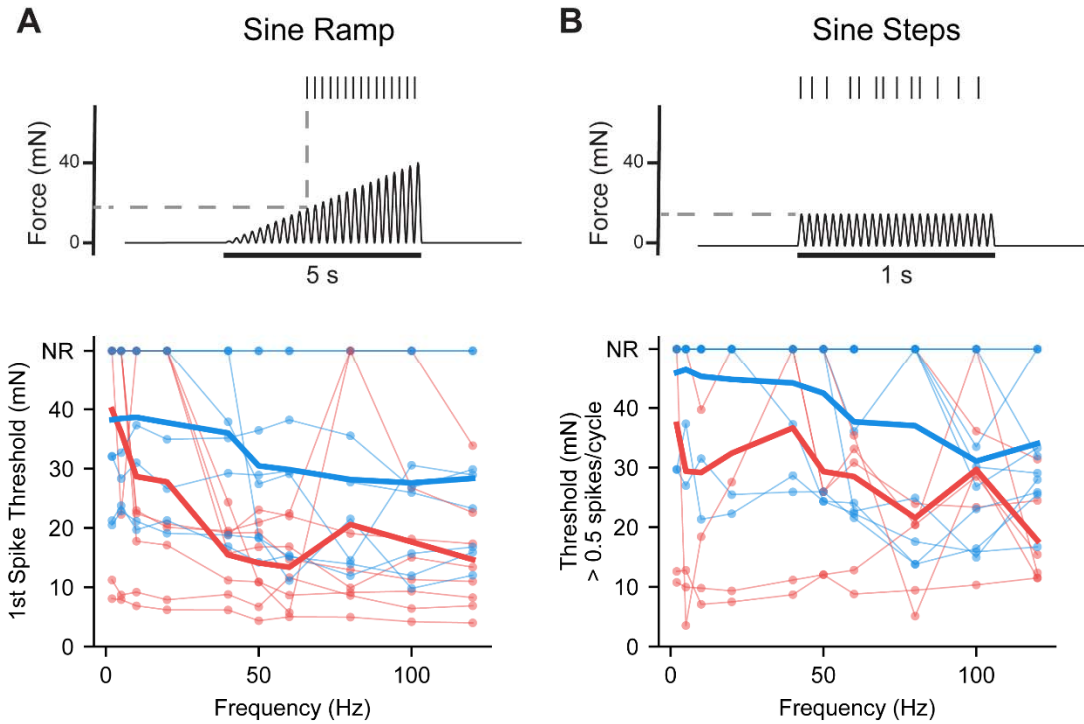


Fig. S8. TrkB⁺ and Ret⁺ Meissner afferents exhibit a wide range of frequency tuning to 2-120 Hz sinusoidal vibrations.

A. Top: Schematic of threshold determination to intensity-ramping sine stimuli. The threshold was measured as the force of the sine envelope at the time of the first action potential.

Bottom: thresholds for individual (connected points) and mean (thick line) TrkB⁺ (blue) and Ret⁺ (red) Meissner afferents. NR: no response.

B. Top: Schematic of threshold determination to a sine-step protocol. Intensities and frequencies were drawn at random, and the intensity at which the Meissner afferent fired greater than 0.5 spikes/cycle was considered the threshold for each frequency. Bottom:

thresholds for individual (connected points) and mean (thick line) TrkB⁺ (blue) and Ret⁺ (red) Meissner afferents. NR: no response.

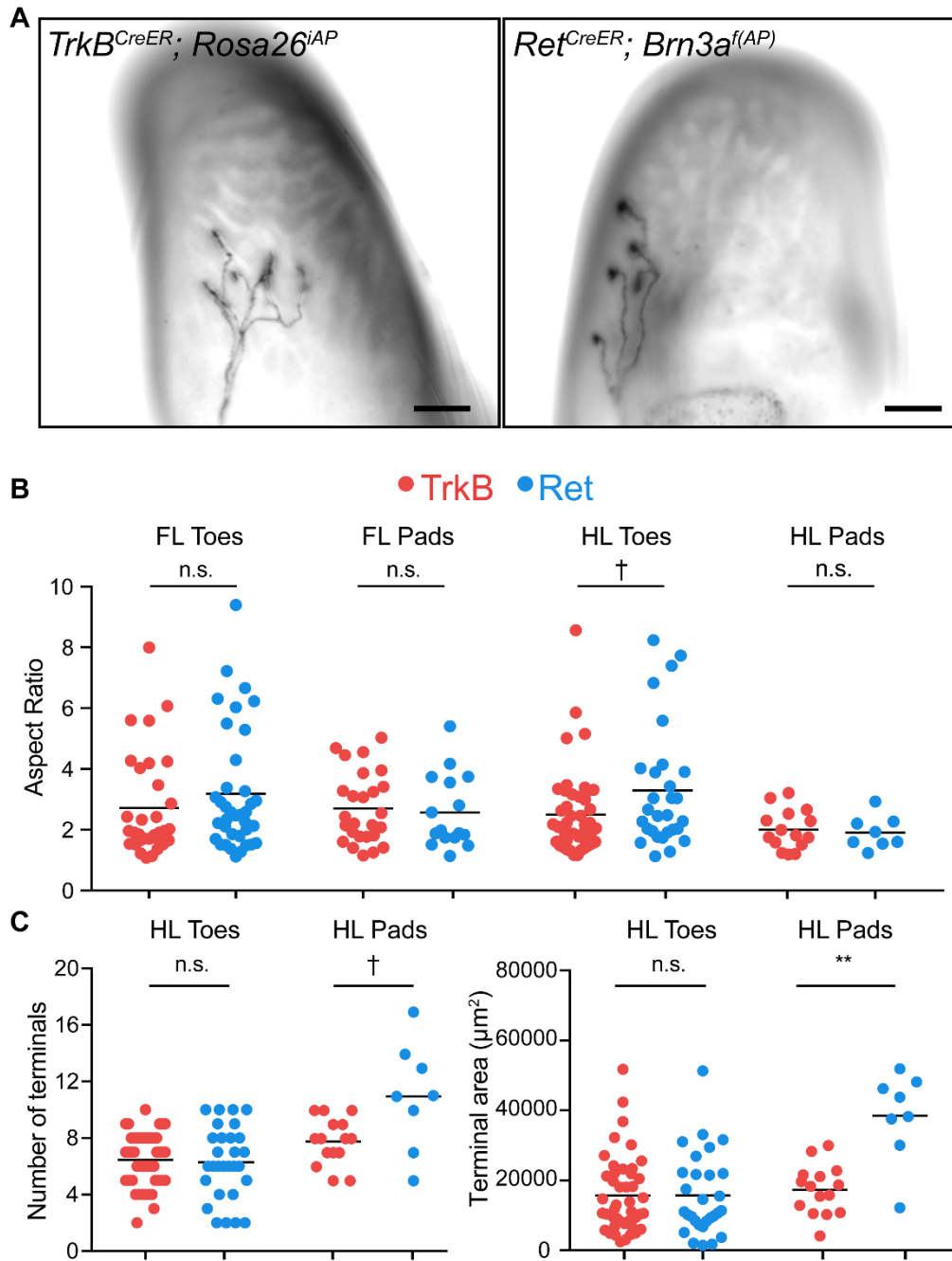


Fig. S9. Measurements of TrkB⁺ and Ret⁺ Meissner afferent morphological receptive fields.

A. Representative images of whole-mount, AP-stained digital pads of a *TrkB^{CreER}; Rosa26^{iAP}* mouse (left) and a *Ret^{CreER}; Brn3a^{f(AP)}* mouse (right), in which TrkB⁺ and Ret⁺ Meissner afferents were sparsely labeled using a low dose of tamoxifen, respectively. Images depict individual

Meissner corpuscle afferents innervating glabrous digital pads. Analysis includes a total 119 individual TrkB⁺ afferent receptive fields (58 forelimb and 61 hindlimb) from 21 mice for and a total of 90 individual Ret⁺ afferent receptive fields (53 forelimb and 37 hindlimb) from 21 mice. (scale bars = 100 μm)

B-C. Aspect ratios (B, major axis/minor axis), number of terminal endings (C, left), and surface areas (C, right) of TrkB⁺ and Ret⁺ Meissner afferent morphological receptive fields measured in *TrkB^{CreER}; Rosa26^{iAP}* or *TrkB^{CreER}; Brn3a^{f(AP)}* mice and *Ret^{CreER}; Rosa26^{iAP}* or *Ret^{CreER}; Brn3a^{f(AP)}* mice. Individual measurements and mean values (black bar) are plotted for each group.

Receptive field quantification plotted here and in Figure 3 includes data from 119 individual TrkB⁺ afferent receptive fields (58 forelimb and 61 hindlimb) from 21 mice and from 90 individual Ret⁺ afferent receptive fields (37 hindlimb and 53 forelimb) from 21 mice. (two-tailed Welch's t-test, mean significantly different: ** p < .01; F-test of the equality of variances, variance significantly different: † p < .05).

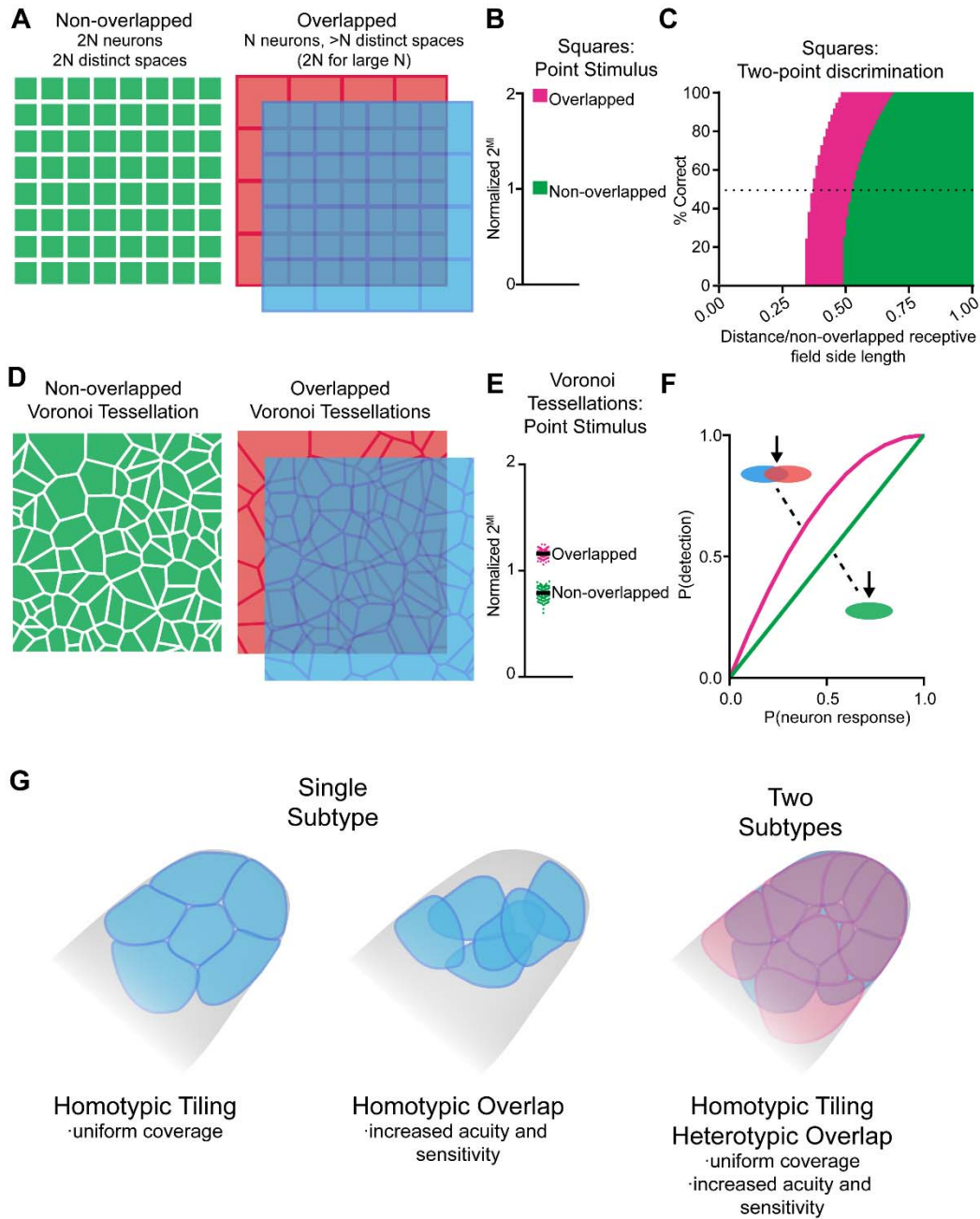


Fig. S10. Computational modeling suggests that heterotypic overlap of homotypically tiled mosaics, like that observed in Meissner corpuscle afferents, enables both uniform skin coverage and enhanced acuity.

A. Schematic demonstrating overlapped grids of homotypically tiled uniform squares (blue and red) and their equivalent non-overlapped grids (green). Overlapped receptive fields provide

greater than N discriminable spaces (approaching $2N$ for large numbers of neurons), while non-overlapped receptive fields would require more neurons with smaller receptive fields to achieve the same resolution (see Methods).

B. Mutual information (MI) between a single pixel stimulus and the responses of simulated grids of uniform squares with overlapped and non-overlapped arrangements. Mutual information was normalized by the number of neurons ($2^{MI}/N$) such that perfect performance of a non-overlapped arrangement should be equal to 1 and perfect performance for an overlapped arrangement should be 2 (see Methods).

C. Two-point discrimination ability of overlapped vs. non-overlapped grids. The two stimuli were 1) a central point and 2) a point shifted by some distance from the central point. For each distance, the point was positioned at all angles between 0 and 2π radians. The percentage of points in which the representation of the central point and the representation of the shifted point were different are plotted for each distance relative to the side lengths of the square neurons of the non-overlapped arrangement (see Methods). For a fair comparison, modeled receptive fields for the overlapped arrangement are larger than for the non-overlapped arrangement to achieve the same total number of neurons.

D. Schematic of non-overlapped (left) and overlapped (right) Voronoi tessellations.

E. Mutual information ($2^{MI}/N$) between a single point stimulus and the responses of overlapped and non-overlapped Voronoi tessellations generated in MATLAB (see Methods for details).

Using 4000 generated tessellations, pairs of tessellations were overlapped to create 2000 overlapped mosaics. The number of neurons, N , was the number of randomly seeded points per arrangement, and MI was normalized by N to allow comparison between arrangements

with different numbers of neurons. A random subset of these results is plotted: The pink circles represent the normalized MI for 100 examples of overlapped tessellations, and the green circles represent the normalized MI for 100 examples of non-overlapped tessellations. Black bars in both cases represent the overall mean.

F. Probability of detection (the probability that at least one neuron responds) plotted as a function of the probability of a single neuron responding to a stimulus within its receptive field. The green line depicts the probability of detection for a single-layered arrangement of homotypically tiled neurons ($P(\text{neuron responds})$). The pink line indicates the probability of detection for a double-layered arrangement of overlapping neurons assuming the neurons are independent ($1-(1-P(\text{neuron responds}))^2$). The probability of detection is greater for an overlapping arrangement at all probabilities between 0 and 1, exclusive.

G. Homotypic tiling of a single subtype of Meissner tactile afferents ensures uniform and complete coverage of the skin surface (left). On the other hand, homotypic overlap can provide higher sensitivity and acuity, but this arrangement comes at the expense of the uniformity and completeness of skin coverage ensured by a tiling mechanism (center). Combining both homotypic tiling and non-redundant heterotypic overlap through the existence of two molecularly distinct subtypes of tactile afferents ensures uniform and complete coverage of the skin while also enabling high acuity and sensitivity, using the fewest neurons (right).

Movie S1

Advillin^{Cre};TrkB^{fllox/+} (control) mouse demonstrating typical sunflower seed eating behavior.

Movie S2

TrkB^{CKO} mouse demonstrating difficulty with opening and eating sunflower seeds.